

Comparison of Polychromatic and Monochromatic X-rays for Imaging

M. Hoheisel¹, P. Bernhardt¹, R. Lawaczeck², and H. Pietsch²

¹ Siemens AG Medical Solutions, Forchheim, Germany

² Schering AG Imaging Diagnostics and Radiopharmaceuticals Research, Berlin, Germany

ABSTRACT

Monochromatic X-rays have been proposed for medical imaging, especially in the mammographic energy range. Our previous investigations have shown that the contrast of objects such as lesions or contrast media can be enhanced considerably by using monochromatic X-rays instead of the common polychromatic spectra. Admittedly, only one specific polychromatic spectrum and one monochromatic energy have been compared so far.

In this work, we investigated the contrast yielded by a series of different X-ray spectra obtained by varying tube voltage and beam filtering. This resulted in spectra of different mean energies and spectral widths. The objects under examination were aqueous solutions containing different chemical elements such as I, Gd, Dy, Yb, and Bi.

A monoenergetic spectrum at 17.5 keV was obtained using a mammographic X-ray tube with a Mo anode and a monochromator equipped with a HOPG crystal. Moreover, we simulated quasi-monoenergetic spectra at different energies and with different widths.

As a result, we demonstrated that in many cases spectra with an energetic width of some keV yield an equivalent contrast to monoenergetic radiation at the same energy. Therefore, the advantage in image contrast of monochromatic X-rays at 17.5 keV over narrow-band polychromatic X-ray spectra obtained by appropriate filtering is only slight. Thus, the additional expenditure on a mammography system with HOPG monochromator that can deliver only a small X-ray dose and the unfavorable slot-scan geometry can be avoided.

Moreover, we carried out simulations of monochromatic versus polychromatic spectra throughout the whole radiographic energy range. We found advantages in using monochromatic X-rays at higher energies and thicker objects that will justify their application for diagnostic imaging in a number of specific cases.

Keywords: Medical X-ray imaging, monochromatic source, Highly Oriented Pyrolytic Graphite (HOPG), spectral width, mammography, signal-difference-to-noise ratio, contrast enhancement, contrast media

1. INTRODUCTION

In the field of medical X-ray imaging, much effort has been directed towards finding an optimum spectrum for every specific diagnostic situation. This includes the choice of the anode material of the X-ray tube, the tube voltage, as well as material and thickness of additional filters¹.

To visualize a certain lesion, the ratio of contrast to noise should be as high as possible, where contrast means the signal difference between lesion and surrounding tissue. Since the absorption coefficient becomes lower with increasing energy, a low energy will deliver high contrast. Unfortunately, with lower energy the patient dose increases while less quanta will reach the detector and be registered. This calls for the use of high energies. It is evident that there is an optimum energy in between. This gives rise to the demand for a monochromatic X-ray source at this very energy. A simulation study on this subject has been conducted for instance by Boone and Seibert².

Up to now, monochromatic X-rays have been produced by synchrotrons or parametric X-ray sources³, which are very expensive and complex methods. Therefore, synchrotron radiation has not found its way into everyday clinical life. The common approach is to use as narrow a continuous spectrum as possible, which is accomplished by absorption filters. Thick filters are extremely useful for this purpose, but are limited by the increase in tube load.

In our previous work⁴ we pursued another approach. We used an ordinary X-ray tube, a highly oriented pyrolytic graphite (HOPG) mirror, and a slit defining the Bragg angle for the desired energy. This arrangement forms a fan beam source. Together with a linear detector we have a slot-scan system. Diekmann et al.⁵ demonstrated that this approach

might be advantageous in some situations. Nevertheless, such a slot-scan system with a monochromator has several drawbacks, such as a quantum flux that is lower by a factor of 20 thus necessitating multiple scans to reach the dose required for a sufficient noise level, or extremely long scanning time leading to motion artifacts. Therefore, we tried to work out whether a well-adapted polychromatic spectrum can yield the same performance as monochromatic X-ray radiation.

2. METHOD

This work is based mainly on simulations. We used a series of different phantoms that span the whole range of medical diagnostic procedures. For the mammographic energy range we used 2 cm to 8 cm thick slabs composed of 25% adipose and 75% glandular tissue. For the radiographic energy range we applied water phantoms of between 10 cm and 44 cm thickness. In each phantom we implanted thin pieces of different materials, i.e. the chemical elements Al, Y, I, Gd, Dy, Yb, and Bi (in order of their atomic numbers 13, 39, 53, 64, 66, 70, and 83, respectively), representing lesions or contrast agents.

We investigated in this study the signal-difference-to-noise ratio (SDNR) of these materials. The SDNR is a well-suited quantity to characterize the contrast behavior of an object, since it is invariant to many image-processing operations, e.g. windowing. As a figure of merit we chose $Q = \text{SDNR}^2/K$ with the air kerma K at the surface of the phantom, because this variable easily allows the comparison of results derived from different measurements. In one case, $Q = \text{SDNR}^2/D$ with the absorbed dose D was used instead.

The simulations included monochromatic X-rays as well as polychromatic spectra. A deterministic simulation yielded the contrast emerging from the different material samples. An additional Monte-Carlo simulation produced the noise figures. Scattered radiation was ignored in the course of this work. Details of the simulations will be published elsewhere⁶. The monochromatic energy E_x was varied over a sufficiently broad spectral range to yield a $Q(E_x)$ function with a maximum.

Other simulations have been carried out using polychromatic spectra which are given by the X-ray tube and filtration parameters (anode material, tube voltage, filter material and thickness). The idea was to substitute the optimal monochromatic radiation with a broader X-ray spectrum at the same mean energy. Then the signal is generated by both the optimum energy and suboptimal spectral contributions. One aim of this study was to evaluate to what extent a broader spectrum can lead to the same or nearly the same SDNR as the monochromatic spectrum.

Furthermore, we carried out measurements on real phantoms. The objects under examination were 10 mm high cuvettes with aqueous solutions containing different chemical elements such as I, Gd, Dy, Yb, and Bi in a concentration of 20 mmol/l each. The measured contrast was defined as the quotient between the signal intensity behind these objects and the signal intensity behind a similar cuvette containing pure water.

The X-ray system for monochromatic imaging was compiled as follows: The basic system was a Siemens Mammomat[®] 300 mammography device, contributing the X-ray tube, the high voltage generator, the operating console, and the mechanical setup. The tube had a molybdenum anode and was operated with 35 kV voltage and 100 mA current in most cases. A permanent pre-filtration of 30 μm Mo was used. Admittedly, we could use only one single monochromatic energy, 17.5 keV, which is the K_α energy of molybdenum. The monochromator could have been tuned to other energies also, but only delivers a sufficiently high quantum flux at the K_α line. The detector was a CCD (Thales TH9570), 4092 x 200 pixels, 54 μm in size in the binning mode.

For the polychromatic spectra we used the same mammography system with its Mo anode without monochromator and varied the tube voltage in the range 23 kV to 35 kV. Extra beam filtering was accomplished by a series of 1 mm to 4 mm thick aluminum sheet enabling us to obtain spectra of different mean energy (17.4 keV to 27.4 keV) and different spectral width listed in Table 1.

The resulting spectra could also be simulated and are plotted in Fig. 1. All spectra show a pronounced peak at the K_α energy of 17.5 keV, a second, smaller peak at the K_β energy of 19.6 keV, and a more or less large continuum up to the maximum energy corresponding to the tube voltage selected. Therefore, the overall spectra are rather broad; giving just the spectral width as a parameter is certainly inadequate to characterize each spectrum.

Table 1

Tube voltage	Al filter thickness	Mean energy	Width
23 kV	1 mm	17.4 keV	1.8 keV
29 kV	1 mm	18.7 keV	2.9 keV
35 kV	1 mm	20.6 keV	4.9 keV
35 kV	2 mm	23.1 keV	5.6 keV
35 kV	3 mm	25.5 keV	5.4 keV
35 kV	4 mm	27.4 keV	4.7 keV

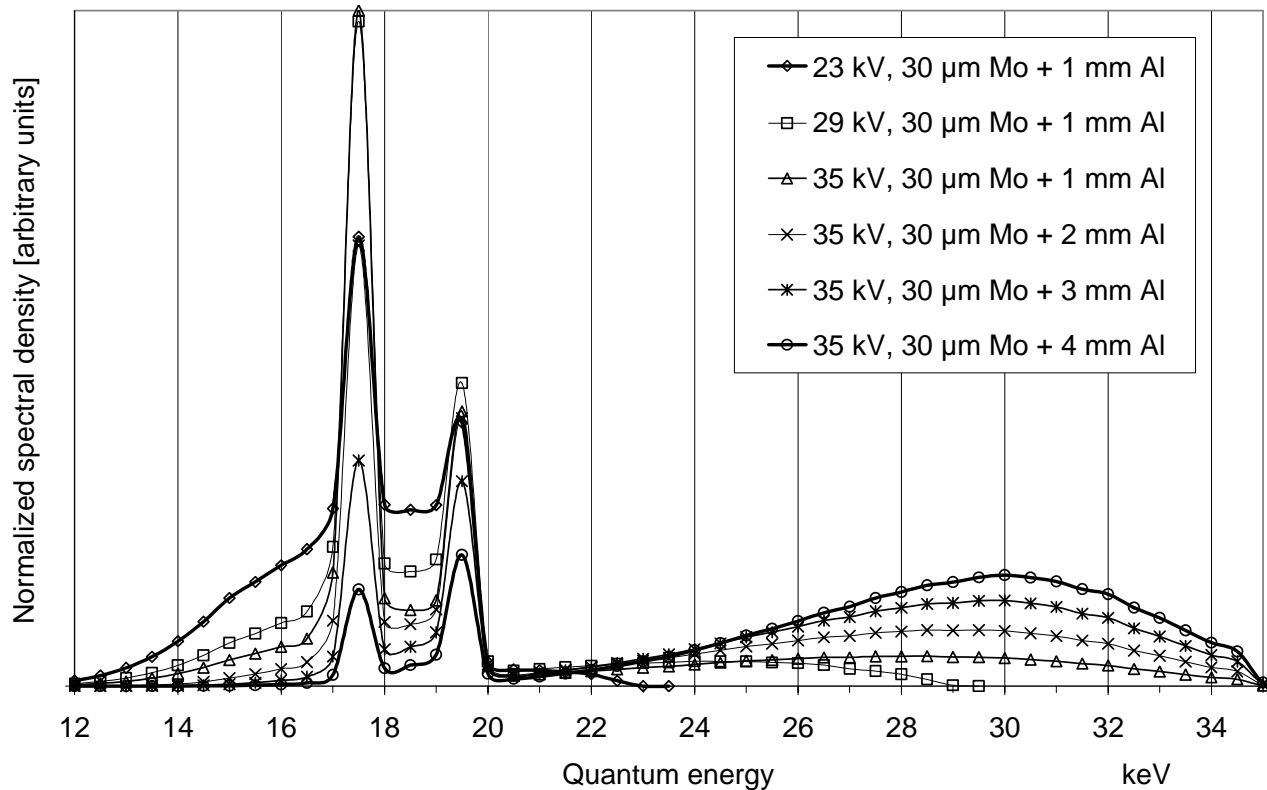


Figure 1: Series of mammographic X-ray spectra from a tube with Mo anode, 30 μm Mo pre-filtration, different tube voltages, and different Al filter thicknesses.

3. SIMULATION RESULTS

First we studied the optimum (monochromatic) X-ray energy E_x for different situations characterized by the phantoms described above. Fig. 2 shows the figure of merit Q as a function of quantum energy for a specific case (Ca sample in a series of mammography phantoms of different thickness). At each thickness a clear maximum is visible which denotes the optimum energy E_x . As a result, the optimum energy E_x can be derived as a function of phantom thickness for a given kind of phantom and contrast sample. This is plotted in the insert of Fig. 2.

From many of these graphs one can compile diagrams such as Fig. 3. In Fig. 3 Q is again plotted as a function of quantum energy for a 20 cm-thick water phantom and various contrast objects which are characterized by their different K_{α} energies. The maxima of these curves, i.e. the optimum quantum energies E_x are ≈ 45 keV for those materials with a K_{α} energy below 45 keV. Contrast objects with $K_{\alpha} > 45$ keV lead to pronounced maxima near their respective K_{α} energies.

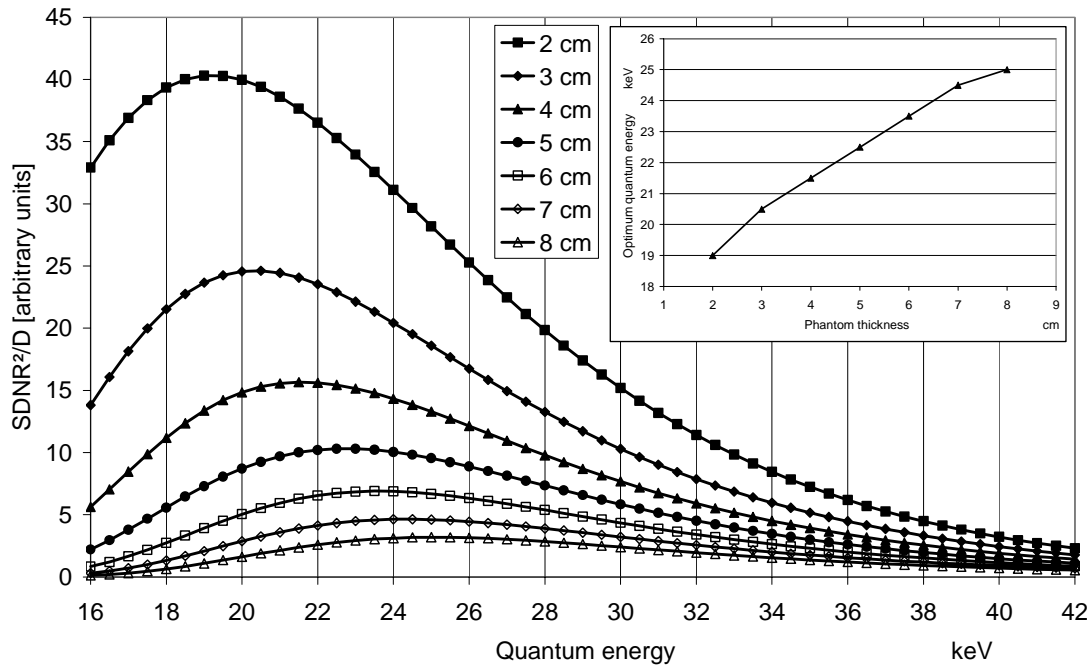


Figure 2: Figure of merit $Q = \text{SDNR}^2/D$ as a function of quantum energy assuming monochromatic X-rays for a calcification in a series of mammography phantoms (25% fatty, 75% glandular tissue) of different thickness. Every curve shows a clear maximum at its optimum energy E_x . The insert shows E_x as a function of phantom thickness.

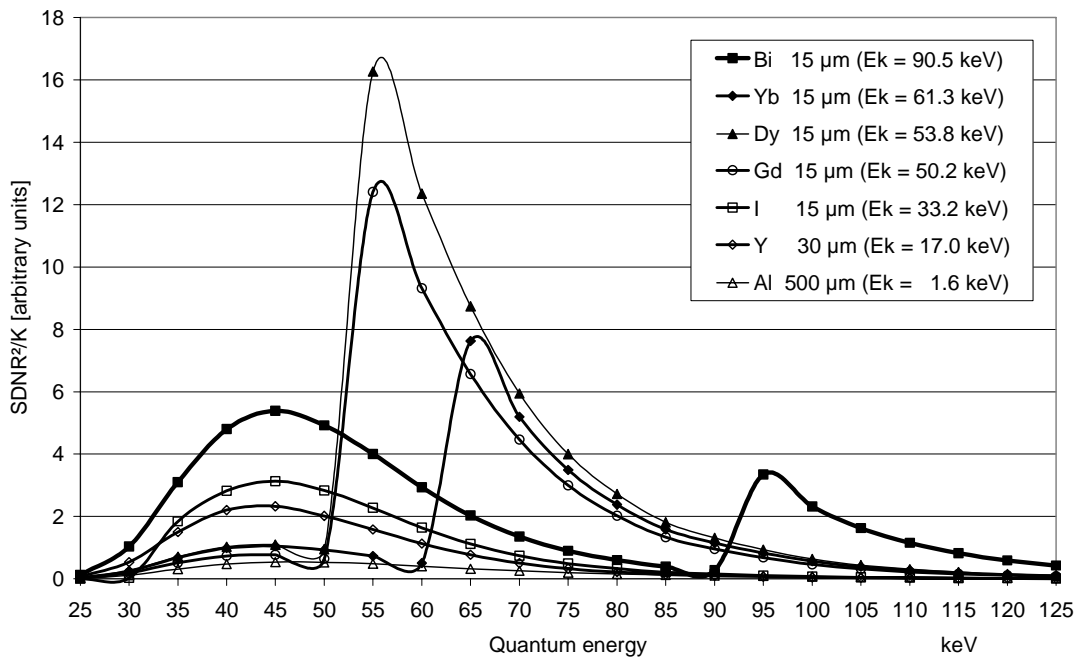


Figure 3: Figure of merit $Q = \text{SDNR}^2/K$ as a function of quantum energy assuming monochromatic X-rays for different contrast objects in a 20 cm-thick water phantom. The curves are guides to the eye. Every curve shows a clear maximum at its optimum energy E_x . If the K-edge energy E_k of the contrast object is above ≈ 45 keV, E_x is found in the vicinity of E_k .

For the simulations using polychromatic spectra we varied the tube voltage from 40 kV to 150 kV in steps of 5 kV. The additional filtration was 0 mm, 0.1 mm, 0.2 mm, 0.3 mm, 0.6 mm, or 0.9 mm for each voltage step. Again, Q was calculated for the same contrast elements as above and different phantom thicknesses. Similar to the results shown in Fig. 3, a maximum can be found for every phantom and contrast object. The X-ray spectrum which produced this maximum was then calculated from the tube voltage and filtration parameters. Fig. 4 is a compilation of these spectra.

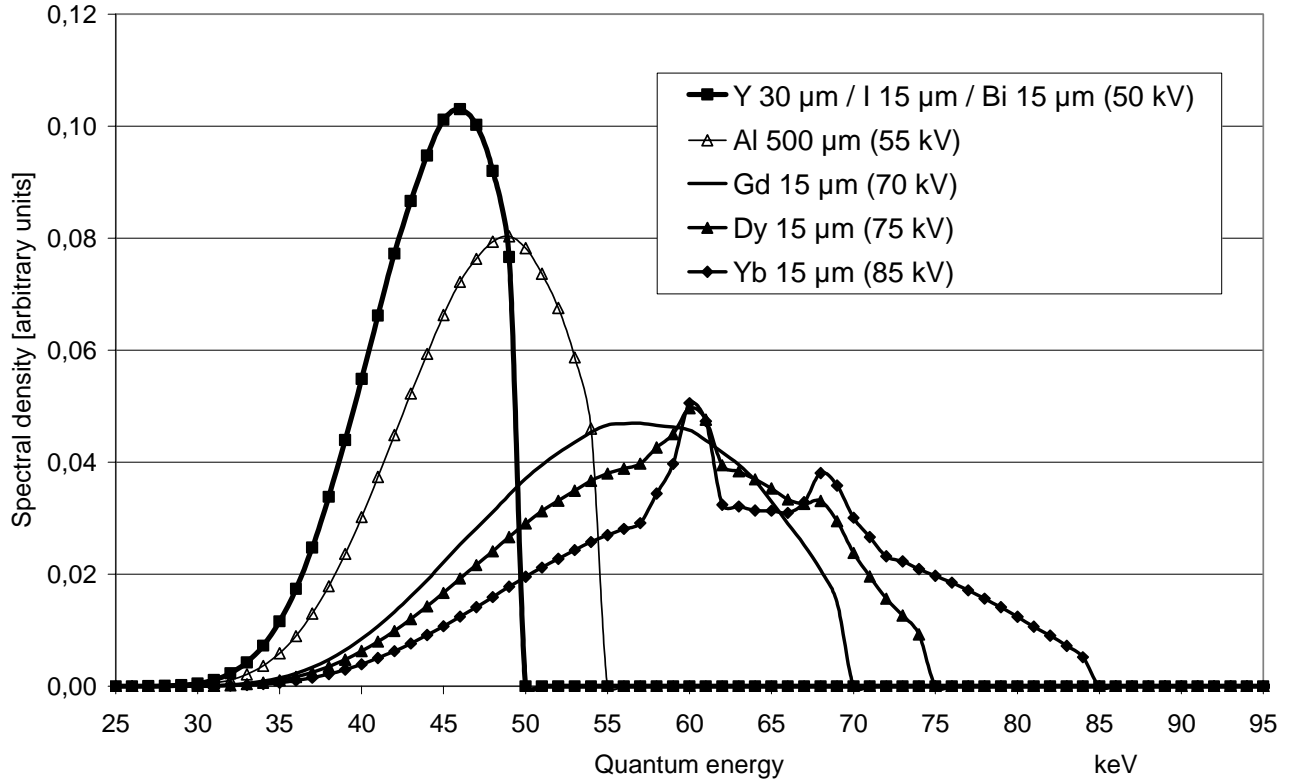


Figure 4: A series of X-ray spectra which were found to yield the optimum figure of merit $Q = \text{SDNR}^2/K$ for the different contrast objects (given in the caption) in a 20 cm-thick water phantom. Although all spectra have been obtained with maximum filter thickness (0.9 mm) their spectral width is rather high.

It is interesting to note that all spectra of Fig. 4 have been obtained with the maximum filter thickness, i.e. 0.9 mm, which is the maximum filter thickness implemented in the Siemens Axiom® X-ray systems. Thicker filters would require a much higher tube power which is currently not available. Thicker filters lead to narrower spectra which come closer to ideal monochromatic spectra.

As long as the tube voltage is kept below 65 kV, the K_{α} emission line of the W anode at 59.3 keV does not play a significant role and the resulting spectra in Fig. 4 consist of a single peak. Higher tube voltages result in rather broad spectra with a pronounced superimposed peak at 59.3 keV and, at even higher voltages, a second peak at 67.2 keV, the K_{β} emission line of W. The consequence of these peaks is that it is impossible to raise the mean energy of the spectrum significantly above 70 keV, even when the tube voltage is set to the highest value we have on-hand, i.e. 150 keV.

The optimum Q values found with monochromatic (Q_{mono}) and polychromatic (Q_{poly}) spectra for the different contrast objects at a 20 cm and, since the optima depend markedly on the phantom thickness, a 40 cm water phantom are listed in Table 2. All polychromatic spectra applied were those shown in Fig. 4, where a filtration of 0.9 mm Cu and different tube voltages had been used. Furthermore, the quotient Q_{poly}/Q_{mono} is given for each case to show in how far Q_{poly} can compete with Q_{mono} . Similar relations between monochromatic and polychromatic radiation on phantoms of different thickness had already been found by Oosterkamp⁷.

Table 2

Contrast object	20 cm water phantom			40 cm water phantom		
	Q monochromatic	Q polychromatic	Q_{poly}/Q_{mono}	Q monochromatic	Q polychromatic	Q_{poly}/Q_{mono}
Al	5.380E+05	4.698E+05	87.3%	7.224E+03	5.252E+03	72.7%
Y	2.326E+06	2.001E+06	86.0%	2.452E+04	1.603E+04	65.4%
I	3.130E+06	2.647E+06	84.6%	3.442E+04	2.251E+04	65.4%
Gd	1.241E+07	6.019E+06	48.5%	1.869E+05	9.937E+04	53.2%
Dy	1.627E+07	6.252E+06	38.4%	2.451E+05	1.177E+05	48.0%
Yb	7.627E+06	2.563E+06	33.6%	1.543E+05	5.184E+04	33.6%
Bi	5.389E+06	4.559E+06	84.6%	1.098E+05	3.932E+04	35.8%

The polychromatic spectra resulting from our simulations are unrealistic from a practical point of view. For all spectra a 0.9 mm Cu filtration was used to make the spectra as narrow as possible. Since a sufficiently high dose is required to produce high-quality radiograms, in most cases no additional filter is used. Table 3 shows the Q values under the assumption that no additional filters have been applied.

Table 3

Contrast object	20 cm water phantom			40 cm water phantom		
	Q monochromatic	Q polychromatic	Q_{poly}/Q_{mono}	Q monochromatic	Q polychromatic	Q_{poly}/Q_{mono}
Al	5.380E+05	2,324E+05	43.2%	7.224E+03	2,580E+03	35.7%
Y	2.326E+06	9,454E+05	40.6%	2.452E+04	6,993E+03	28.5%
I	3.130E+06	1,177E+06	37.6%	3.442E+04	9,874E+03	28.7%
Gd	1.241E+07	2,610E+06	21.0%	1.869E+05	4,024E+04	21.5%
Dy	1.627E+07	2,894E+06	17.8%	2.451E+05	4,667E+04	19.0%
Yb	7.627E+06	1,217E+06	16.0%	1.543E+05	2,186E+04	14.2%
Bi	5.389E+06	2,164E+06	40.2%	1.098E+05	2,242E+04	20.4%

Taking practical boundary conditions into account, even well-adapted polychromatic spectra deliver Q values roughly a factor of two lower than narrow polychromatic spectra, and up to a factor of seven lower than the Q values that would be achieved with monochromatic X-rays, as can be seen from Table 3.

4. EXPERIMENTAL RESULTS

For the experimental investigations we followed a slightly different approach since we had to use a fixed monochromatic energy of 17.5 keV. We used the spectra denoted in Table 1 and Fig. 1. Then we determined Q for I, Gd, Dy, Yb, and Bi as a function of the mean energy (Fig. 5). Q increases when the mean energy is lowered and reaches almost the same value as in the monochromatic case.

The different contrast objects were 10 mm high cuvettes with aqueous solutions as explained above. Therefore, the thickness of the phantom was held constant at 1 cm and not varied as in the simulations. The contrast for all elements increased according to their attenuation coefficients, i.e. with the atomic number of the contrasting element from I to Bi.

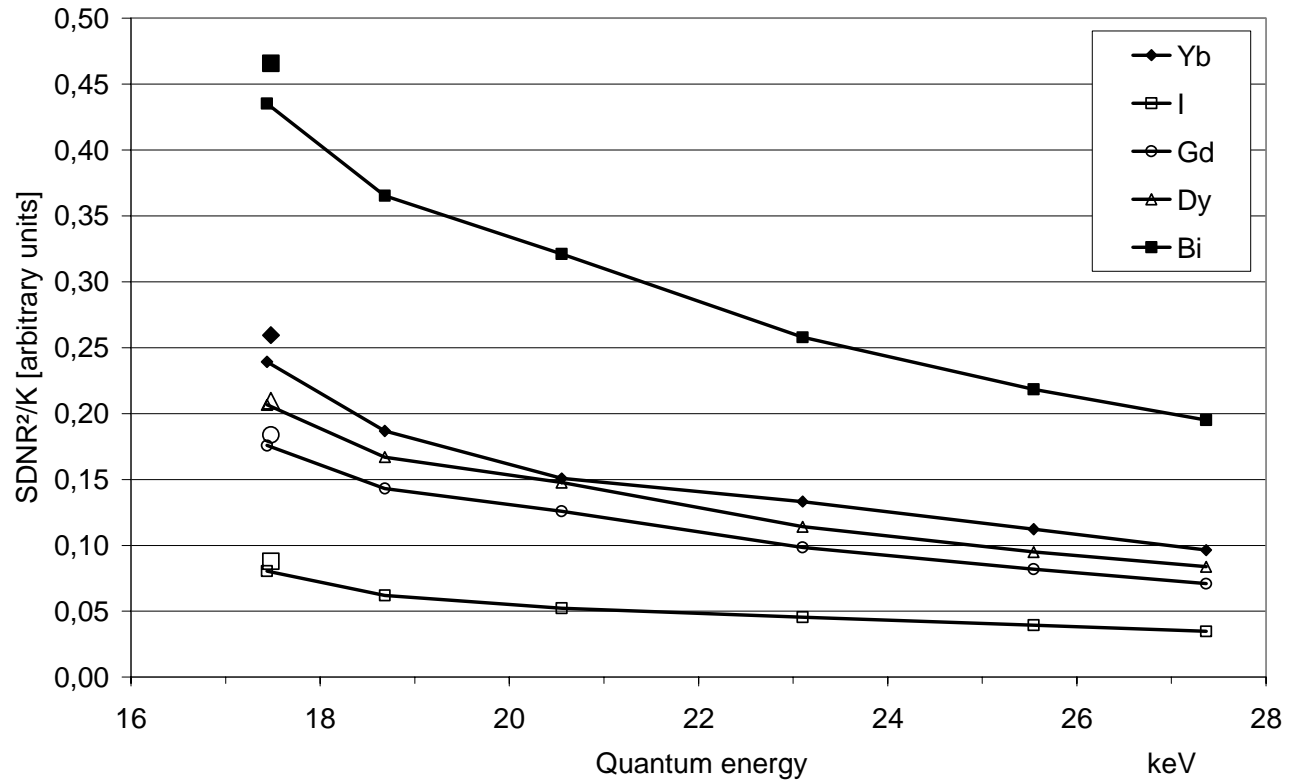


Figure 5: Figure of merit $Q = \text{SDNR}^2/K$ as a function of the mean energy of different polychromatic spectra. The objects consisted of aqueous solutions of I, Gd, Dy, Yb, and Bi with $20 \mu\text{mol}/\text{cm}^2$ each. The corresponding Q values for the monochromatic case are plotted at 17.5 keV in larger symbols. With a mean energy of 17.5 keV nearly the same Q values can be reached.

5. CONCLUSIONS

In this study we investigated the optimum energy of monochromatic X-rays for medical diagnostic applications. The achievable SDNR values were compared with those of appropriate polychromatic spectra.

Simulations with monochromatic spectra confirm the well-known fact that in most cases there is an optimum quantum energy for a good $Q = \text{SDNR}^2/K$. Fortunately, in mammography Q shows a rather broad maximum as can be seen from Fig. 2. Deviations of ± 2 keV will reduce SDNR by some 10% which often might be tolerable.

As a general trend, thicker objects require higher quantum energies for sufficient penetration. However, depending on the details of interest present in these objects, e.g. contrast media, the optimum energy may be different. The optimum energy results primarily from the thickness of the background object (see Al, Y, and I in Fig. 3). If the K-edge energy of the dominating chemical element in the detail is below this energy, the optimum energy is not noticeably changed. With a higher K-edge energy a significantly better Q value can be obtained at a quantum energy slightly above this K-edge energy.

Using polychromatic spectra one can yield similar SDNR values as long as the maxima of Q as a function of quantum energy are sufficiently broad and the polychromatic spectra are accordingly narrow. This is generally the case at low energies such as applied in mammography. Table 2 shows that the Q values are only some 10% to 30% lower for a 20 cm and a 40 cm thick phantom, and for monochromatic compared to polychromatic X-rays, respectively.

If contrast media with a higher Z are present, the optimum shifts to a much higher energy, as can be seen in Fig. 3. This calls for a polychromatic spectrum at this higher energy. Unfortunately, in this energy range the X-ray spectra are dominated by the K_{α} and K_{β} emission lines of W. The total spectra become rather broad and mean energies significantly above 70 keV are not feasible (see Fig. 4).

These relations lead to an interesting finding. Bi is a material with a very high Z of 83 and a K-edge energy of 90.5 keV. Therefore, the optimum quantum energy for a phantom with a Bi detail is around 95 keV. One would expect that the optimum polychromatic spectrum for Bi would require a very high tube voltage. Conversely a tube voltage of only 50 kV leads to the best Q value. The explanation is that even the highest tube voltage available cannot push the mean energy of the spectrum high enough. That is why the optimum polychromatic spectrum for Bi is found to have a mean energy of only 45 keV which coincidences with the second (lower) maximum of the Bi curve in Fig. 3.

In general it was found that using thick absorption filters next to the tube is beneficial in all cases. Unfortunately, this is limited by the maximum tube load the system can deliver.

The experiments we carried out at a monochromatic energy of 17.5 keV and with polychromatic spectra produced by a mammography system confirmed that with subtly adapted polychromatic spectra one can yield nearly the same SDNR as in the monochromatic case. Therefore, using a sophisticated monochromatic scanning setup for mammography appears not to be justified.

Under radiographic conditions the situation is similar. However, there is some benefit from using monochromatic X-rays instead of polychromatic spectra. With monochromatic X-rays of appropriate energy, Q values of about a factor of two to three higher than for optimized polychromatic spectra might be reached, as can be seen from Table 2. Admittedly, it is much more complicated to produce monochromatic radiation at these high energies (> 40 keV). The Bragg angles become very small which results in very long system setups (several meters) that will not fit in a clinical environment. Moreover, cutting out a single energy out of the bremsstrahlung spectrum is not effective and leads to a low quantum flux and extremely long exposure times. Finally, a scanning setup is necessary to utilize monochromatic radiation.

ACKNOWLEDGEMENT

We would like to thank M. Murphy for critically reading the manuscript.

REFERENCES

1. M. Säbel, H. Aichinger, „Recent developments in breast imaging“, *Physics in Medicine and Biology* **41**, 315-368, 1996
2. J. M. Boone, J. A. Seibert, „A comparison of mono- and poly-energetic X-ray beam performance for radiographic and fluoroscopic imaging“, *Medical Physics* **21**, 1853-1863, 1994
3. M. A. Piestrup, X. Wu, V. V. Kaplan, S. R. Uglov, J. T. Cremer, D. W. Rule, R. B. Fiorito, “A design of mammography units using a quasimonochromatic X-ray source”, *Review of Scientific Instruments* **72**, 2159, 2001
4. M. Hoheisel, R. Lawaczek, H. Pietsch, V. Arkadiev, “Advantages of monochromatic X-rays for imaging”, *Proceedings of SPIE* **5745**, 1087-1095, 2005
5. F. Diekmann, S. Diekmann, K. Richter, U. Bick, T. Fischer, R. Lawaczek, W. R. Press, K. Schon, H. J. Weinmann, V. Arkadiev, A. Bjeoumikhov, N. Langhoff, J. Rabe, P. Roth, J. Tilgner, R. Wedell, M. Krumrey, U. Linke, G. Ulm, B. Hamm, „Near monochromatic X-rays for digital slot-scan mammography: initial findings“, *European Radiology* **14**, 1641-1646, 2004
6. P. Bernhardt, T. Mertelmeier, M. Hoheisel, „X-ray spectrum optimization of full-field digital mammography: simulation and phantom study“, submitted to *Medical Physics*
7. W. J. Oosterkamp, “Monochromatic X-rays for medical fluoroscopy and radiography”, *Medica Mundi* **7**, 68-77, 1962